Topological quantization of the spin Hall effect in two-dimensional paramagnetic semiconductors

Xiao-Liang Qi,[1] Yong-Shi Wu,[2,1] and Shou-Cheng Zhang[3,1]

[1]*Center for Advanced Study, Tsinghua University, Beijing 100084, China*
[2]*Department of Physics, University of Utah, Salt Lake City, Utah 84112-0830, USA*
[3]*Department of Physics, McCullough Building, Stanford University, Stanford, California 94305-4045, USA*

We propose models of two-dimensional paramagnetic semiconductors where the intrinsic spin Hall effect is exactly quantized in integer units of a topological charge. The model describes a topological insulator in the bulk and a "holographic metal" at the edge, where the number of extended edge states crossing the Fermi level is dictated by (exactly equal to) the bulk topological charge. We also demonstrate the spin Hall effect explicitly in terms of the spin accumulation caused by the adiabatic flux insertion.

I. INTRODUCTION

The intrinsic spin Hall effect is a novel phenomenon in condensed matter physics, where a dissipationless spin current is proposed to be induced by an external electric field. The effect has been theoretically predicted both in *p*-doped semiconductors with Luttinger type of spin-orbit (SO) coupling[1] and in *n*-doped semiconductors with Rashba type of SO coupling.[2] After these initial proposals, the issue of the stability of the intrinsic spin Hall effect was intensely debated theoretically. It is now broadly believed that the vertex corrections due to impurity scattering exactly cancel the intrinsic spin Hall effect in the *n*-type Rashba model,[3–5] while the vertex corrections vanishes for the *p*-type Luttinger[6] and Rashba [7] models. In the latter case, the impurity scattering does not affect the intrinsic spin Hall effect in the clean limit. This conclusion is also supported by extensive numerical calculations.[8] Remarkably, the spin Hall effect has been experimentally observed.[9,10] The experiment of Ref. 10 was carried out in a two-dimensional hole gas (2DHG) in the clean limit, and the effect is likely of intrinsic nature.

The next logical question in the study of the emerging field of the spin Hall effect concerns the dissipationless nature of the transport and possible quantization of the spin Hall conductivity. Murakami, Nagaosa, and Zhang proposed that the intrinsic spin Hall effect can even exist in insulators where the Fermi level lies within a band gap.[11] In a spin Hall insulator, there is no charge current but spin currents, and the transport can be completely dissipationless. Bernevig and Zhang have proposed that the spin Hall effect can be quantized in two dimensions.[12] In their proposal, the Landau levels arise from the gradient of the strain, rather than the magnetic field.

In the present paper, we propose a realization of the quantum spin Hall effect (QSHE) by specializing the spin Hall insulator model of Ref. 11 to two dimensions. In the presence of mirror symmetry with respect to the *xy* plane, the system is shown to be a topological insulator characterized by a momentum-space winding number $n \in \mathbb{Z}$, with spin Hall transport carried by gapless edge states in a cylindrical geometry, in a way similar to the quantum (charge) Hall system. The evolution of the edge states owing to the adiabatic flux insertion can be traced by following the Laughlin-Halperin argument for the integer quantum Hall effect (IQHE),[13–15] and it can be related explicitly to the spin accu-

mulation at the boundary. Our model therefore describes a bulk topological insulator and a "holographic metal" at the boundary, where the edge transport properties precisely encode the bulk topological invariant.

The rest of this paper is organized as follows. In Sec. II we introduce a systematic description of the quantum anomalous Hall effect (QAHE) in the most general two-band model in two dimensions that realizes the charge QHE without an external magnetic field. It also provides a helpful mathematical preparation for understanding the QSHE. In Sec. III we show how the QSHE emerges in a two-dimensional spin Hall insulator with an "inverted" band structure. Finally, Sec. IV is devoted to conclusions and a discussion.

II. QUANTIZED ANOMALOUS HALL EFFECT

To understand the topological quantization of the spin Hall effect, we shall first introduce a general class of 2D models, called quantum anomalous Hall insulators, in which the charge Hall effect is topologically quantized in the absence of an external magnetic field.

Historically, the first example of the QAHE was introduced by Haldane,[16] which is a tight-binding model defined on a honeycomb lattice with next-nearest-neighbor hopping and staggered flux. (Recently, Kane and Mele generalized Haldane's model and discussed the QSHE.[17]) Similar to the usual quantum Hall effect, the QAHE is also a consequence of momentum-space topology[18] and is robust against local perturbations. We will show the topological nature of the spin Hall conductance in our general two-band model explicitly by a Kubo formula calculation.

The most general two-band Hamiltonian describing a 2D noninteracting system can be expressed in the following form:

$$H = \sum_{\mathbf{k}} H(\mathbf{k}), \quad H(\mathbf{k}) = \epsilon(\mathbf{k}) + V d_\alpha(\mathbf{k}) \sigma^\alpha, \tag{1}$$

where σ^α ($\alpha = 1, 2, 3$) are the three Pauli matrices and $\mathbf{k} = (k_x, k_y)$ stands for the Bloch wave vector of the electron. The two bands may stand for different physical degrees of freedom depending on the context. If they are the components of a spin-1/2 electron, $d_\alpha(\mathbf{k})$ describe the spin-orbit coupling. If they correspond to the orbital degrees of free-

doms, then $d_\alpha(\mathbf{k})$ describe the hybridization between bands. The discussion below is completely independent of the physical interpretation of the Hamiltonian (1) and leads to a general understanding for the conditions for the QAHE.

The Hamiltonian (1) can be easily diagonalized to obtain the two-band energy spectrum as $E_\pm(\mathbf{k}) = \epsilon(\mathbf{k}) \pm V d(\mathbf{k})$, in which $d(\mathbf{k})$ is the norm of the three-vector $d_\alpha(\mathbf{k})$. The Hall conductivity can be calculated using the standard Kubo formula to be

$$\sigma_{xy} = \lim_{\omega \to 0} \frac{i}{\omega} Q_{xy}(\omega + i\delta),$$

$$Q_{xy}(i\nu_m) = \frac{1}{\Omega\beta} \sum_{\mathbf{k},n} \mathrm{tr}[J_x(\mathbf{k}) G(\mathbf{k}, i(\omega_n + \nu_m)) J_y(\mathbf{k}) G(\mathbf{k}, i\omega_n)],$$
(2)

with the current operator $(i,j=x,y)$

$$J_i(\mathbf{k}) = \frac{\partial H(\mathbf{k})}{\partial k_i} = \frac{\partial \epsilon(\mathbf{k})}{\partial k_i} + V \frac{\partial d_\alpha(\mathbf{k})}{\partial k_i} \sigma^\alpha$$
(3)

and $G(\mathbf{k}, i\omega_n)$ the Matsubara Green function.

From Eqs. (2) and (3), the Hall conductivity can be calculated straightforwardly. The details of this calculation are given in the Appendix, with the resulting σ_{xy} given by

$$\sigma_{xy} = \frac{1}{2\Omega} \sum_{\mathbf{k}} \frac{\partial \hat{d}_\alpha(\mathbf{k})}{\partial k_x} \frac{\partial \hat{d}_\beta(\mathbf{k})}{\partial k_y} \hat{d}_\gamma \epsilon^{\alpha\beta\gamma} (n_+ - n_-)(\mathbf{k}),$$
(4)

where $\hat{d}_\alpha(\mathbf{k}) = d_\alpha(\mathbf{k})/d(\mathbf{k})$ is the unit vector along the direction of $d_\alpha(\mathbf{k})$. $\hat{d}_\alpha(\mathbf{k})$ is singular if $d(\mathbf{k}) = \sqrt{d_\alpha(\mathbf{k})d^\alpha(\mathbf{k})}$ vanishes for some $\mathbf{k}$. However, here and below we are always interested in the insulating models, in which a full gap opens between the two bands $E_+(\mathbf{k})$ and $E_-(\mathbf{k})$; thus, $E_+(\mathbf{k}) - E_-(\mathbf{k}) = 2Vd(\mathbf{k}) > 0$ for all $\mathbf{k}$. The gap opening condition is written explicitly as

$$\min_{\mathbf{k} \in \mathrm{BZ}} E_+(\mathbf{k}) > \max_{\mathbf{k} \in \mathrm{BZ}} E_-(\mathbf{k}).$$
(5)

In this case, the system becomes a bulk insulator when the chemical potential lies inside the gap, which implies $n_-(\mathbf{k}) \equiv 1$ and $n_+(\mathbf{k}) \equiv 0$ for all $\mathbf{k}$ at zero temperature. Under such condition and taking the thermodynamic limit, the Hall conductivity (4) can be simplified to

$$\sigma_{xy} = -\frac{1}{8\pi^2} \int\!\!\int_{\mathrm{FBZ}} dk_x dk_y \, \hat{\mathbf{d}} \cdot \partial_x \hat{\mathbf{d}} \times \partial_y \hat{\mathbf{d}},$$
(6)

which is a topological invariant defined on the first Brillouin zone (FBZ), independent of the details of the band structure parameters.[19] Considering $\hat{\mathbf{d}}(\mathbf{k}): T^2 \to S^2$ as a mapping from the Brillouin zone to the unit sphere, the integrand $\hat{\mathbf{d}} \cdot \partial_x \hat{\mathbf{d}} \times \partial_y \hat{\mathbf{d}}$ is simply the Jacobian of this mapping. Thus the integration over it gives the total area of the image of the Brillouin zone on S^2, which is a topological winding number with quantized value $4\pi n, n \in \mathbb{Z}$. Thus the conductivity σ_{xy} is always quantized as $\sigma_{xy} = -n/2\pi$ when the mapping covers S^2 n times. A schematic picture of a typical $\hat{\mathbf{d}}(\mathbf{k})$ configura-
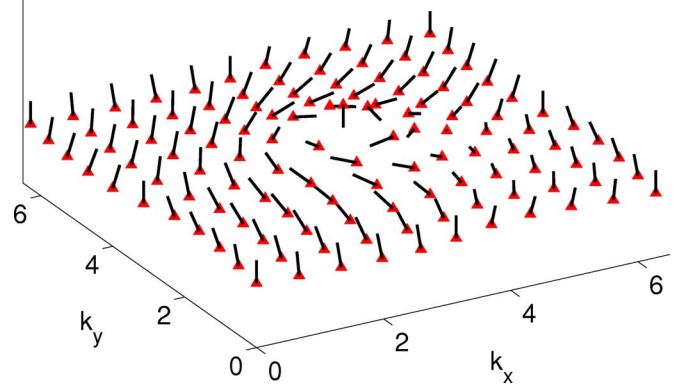

FIG. 1. (Color online) The Skyrmion configuration of $\hat{\mathbf{d}}(\mathbf{k})$ in the Brillouin zone of the system (7) with $c=1$, $e_s=3.7$, and $n=1$. The vector $\hat{\mathbf{d}}(\mathbf{k})$ starts from the north pole at the center of Brillouin zone and ends at the south pole at the zone boundary after covering the unit sphere once.

tion with winding number $n=1$ is shown in Fig. 1. Although the single-electron states in this system are very different from the Landau levels in the usual IQHE, the quantizations of the conductivity in these two systems share the same topological origin, which can be understood as Berry's phase in $\mathbf{k}$ space. The exact formula (6) plays a key role for the QAHE which is similar to that of the Thouless–Kohmoto–Nightingale—den Nijs formula in the Landau-level problem.[18,20] Consequently, both of them are robust against weak disorder due to the topological reason,[21] which is well known for the IQHE case. The general relationship between the momentum-space topology and the quantization of physical responses has been discussed extensively by Volovik in Ref. 22.

For an explicit discussion of the QAHE and the characteristics of edge states, we consider the following choice of $d_a(\mathbf{k})$ as an example:

$$d_x = \sin k_y, \quad d_y = -\sin k_x,$$

$$d_z = c(2 - \cos k_x - \cos k_y - e_s).$$
(7)

When V/t in Hamiltonian (1) is large enough, the insulator condition (5) is satisfied and the Hall conductivity can be shown to be

$$\sigma_{xy} = \begin{cases} 1/2\pi, & 0 < e_s < 2, \\ -1/2\pi, & 2 < e_s < 4, \\ 0, & e_s > 4 \text{ or } e_s < 0, \end{cases}$$
(8)

where the parameter c is taken to be positive. Physically, this model can be understood as a tight-binding model describing some magnetic semiconductor with Rashba-type SO coupling, spin-dependent effective mass, and a uniform magnetization in the z direction. The experimental realization of such a QAHE will be discussed in future works.

To show the behavior of edge states, one can define such a Hamiltonian on a strip with the periodic boundary condition in the y direction and open boundary condition in the x direction, with vanishing wave function at $x=0, L+1$. In this
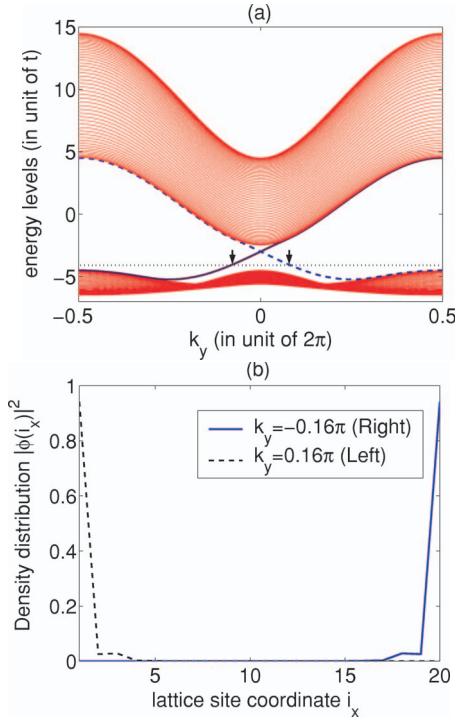
FIG. 2. (Color online) (a) Energy spectrum of the QAHE system (7) when the open boundary condition is imposed in x-direction. The parameters are $c=1, t/V=1/3, e_s=0.5$. The solid and dashed lines between two energy bands stand for the edge states at the right and left edge, respectively. The horizontal dotted line shows a typical chemical potential inside the gap. The two arrows mark the two gapless edge excitation with momentum $k_y = \pm 0.16\pi$. (b) the density distribution of the two edge states at fermi surface, calculated for a 50×50 lattice.

case the Bloch wave vector k_y is a good quantum number and the single-particle energy is a function $E_m(k_y)$ ($m=1, \ldots, 2L$). A typical energy spectrum is shown in Fig. 2. For a given k_y, there are $2L$ states; two of these are localized, while the rest are extended. When the Fermi level lies in the bulk energy gap (as represented in Fig. 2 by a horizontal dotted line), the only gapless excitations are edge states. Similar to the usual IQHE case, the edge states have a definite chirality. In the present case, the state localized at the left edge moves with velocity $v_y < 0$ and that at the right edge with $v_y > 0$. This can be seen directly from the dispersion relation of the edge states. More generally, when $\sigma_{xy} = n/2\pi$, there are $|n|$ chiral edge states on each edge.

III. QUANTUM SPIN HALL EFFECT

Besides its interest in its own right, the above discussions of the QAHE also serve as a natural introduction to the QSHE. In fact, as we shall see, the QSHE can be understood as two copies of the QAHE; each breaks time-reversal symmetry while the whole system remains invariant under time reversal. In particular, let us consider the light-hole (LH) and heavy-hole (HH) bands in a semiconductor which can be described by the Luttinger model:[23]

$$H(\mathbf{k}) = \frac{\gamma_1 + \frac{5}{2}\gamma_2}{2m}\mathbf{k}^2 + \frac{\gamma_2}{m}(\mathbf{S} \cdot \mathbf{k})^2, \quad (9)$$

where the three components of $\mathbf{S}$ stand for the 4×4 angular momentum matrices of a $J=3/2$ electron. According to Ref. 24, such a 4×4 Hamiltonian can be reexpressed by introducing five Dirac Γ matrices $\Gamma^a = \xi_a^{ij}\{S^i, S^j\}$, $a=1, 2, \ldots, 5$, as

$$H(\mathbf{k}) = \epsilon(\mathbf{k}) + V d_a(\mathbf{k})\Gamma^a, \quad (10)$$

with

$$\epsilon(\mathbf{k}) = \frac{\gamma_1}{2m}\mathbf{k}^2, \quad V = \frac{\gamma_2}{m},$$

$$d_1 = -\sqrt{3}k_y k_z, \quad d_2 = -\sqrt{3}k_x k_z,$$

$$d_3 = -\sqrt{3}k_x k_y, \quad d_4 = -\frac{\sqrt{3}}{2}(k_x^2 - k_y^2),$$

$$d_5 = -\frac{1}{2}(2k_z^2 - k_x^2 - k_y^2),$$

and the matrices Γ^a form the SO(5) Clifford algebra $\{\Gamma^a, \Gamma^b\} = 2\delta^{ab}$. [More details about the SO(5) representation of the Luttinger model can be found in Appendix A of Ref. 24.] By using the Clifford algebra, the Hamiltonian (10) can be diagonalized to obtain the doubly degenerate eigenvalues

$$E_\pm(\mathbf{k}) = \epsilon(\mathbf{k}) \pm V\sqrt{d_a d^a(\mathbf{k})} = \frac{\gamma_1 \pm 2\gamma_2}{2m}\mathbf{k}^2. \quad (11)$$

In the present work, we will focus on the spin Hall insulators described by $\gamma_2 > \gamma_1/2$ (Ref. 11) and specialize it to two dimensions. When the semiconductor described by the Hamiltonian (10) is made into a quantum well in the z direction, the effective Hamiltonian can be obtained by adding a potential well term $U(z)$ to the original Luttinger Hamiltonian. When $U(z)$ is narrow enough, the system can be considered as quasi-2D in the low-energy sector, for which one can write down a two-dimensional effective Hamiltonian H_{2D}. The simplest way to obtain H_{2D} is by replacing k_z and k_z^2 in the original Hamiltonian (10) by their average in the lowest subband $\langle k_z \rangle$ and $\langle k_z^2 \rangle$, respectively. When the potential is symmetric, $U(z) = U(-z)$, the parity symmetry with respect to the x-y plane is respected and thus $\langle k_z \rangle = 0$, which means $d_1 = d_2 \equiv 0$, and the 2D Hamiltonian can be simplified to

$$H_{2D} = \epsilon(\mathbf{k}) + V d_\alpha(\mathbf{k})\Gamma^\alpha \quad (\alpha = 3, 4, 5),$$

$$d_3 = -\sqrt{3}k_x k_y, \quad d_4 = -\frac{\sqrt{3}}{2}(k_x^2 - k_y^2),$$

$$d_5 = -\frac{1}{2}(2e_s - k_x^2 - k_y^2), \quad (12)$$

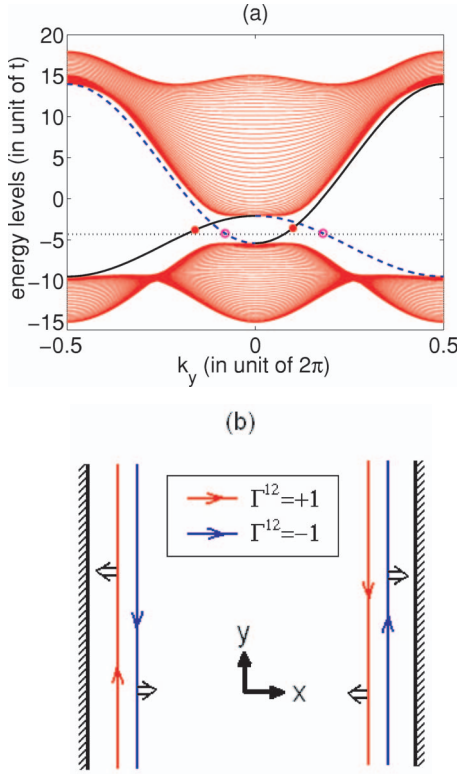with $e_s \equiv \langle k_z^2 \rangle$ and $\mathbf{k} = (k_x, k_y)$.

FIG. 3. (Color online) (a) The energy spectrum in the case (18) with $t/V=4$ and $e_s=0.5$. The isolated solid lines stand for the (doubly degenerate) edge states, and the dashed line indicates a typical in-gap Fermi energy (with $\mu=-4.2t$). Each crossing of the Fermi energy and the edge-state spectrum defines two edge states on left and right boundary with opposite value of Γ^{12}. The solid and open circles near a Fermi level mark the particle and hole edge excitations induced by adiabatic flux insertion. (See the text for details.) (b) Schematic picture of the edge states. Each red (blue) line stands for an edge state with $\Gamma^{12}=+1(-1)$. The double arrow shows the pseudo spin orientation of the current carried by the corresponding edge state when an electric field is applied in the y direction. For simplicity, only one edge state with a definite Γ^{12} eigenvalue on each edge is drawn.

Noticing that Γ_α ($\alpha=3,4,5$) form a reducible representation of an SO(3) Clifford subalgebra, it is natural to see the similarity of the Hamiltonian (10) to the two-component one (1) proposed in the previous section. To see such a similarity explicitly, define

$$\Gamma^{ab} = [\Gamma^a,\Gamma^b]/2i \quad (a,b=1,2,\dots,5);$$

then,

$$[\Gamma^{12},\Gamma^\alpha] = 0(\alpha=3,4,5) \Rightarrow [\Gamma^{12},H_{2d}] = 0. \quad (13)$$

Therefore, Γ^{12} serves as a "conserved spin quantum number" even in the presence of the SO coupling. The eigenvalues of Γ^{12} are ±1 both with double degeneracy, and Γ^{12} and all of Γ^α ($\alpha=3,4,5$) can be block diagonalized simultaneously. Since they form a representation of SO(3) Clifford algebra, the new expression of Γ^a in the diagonal representation of Γ^{12} can always be chosen as

$$\Gamma^{12} = \begin{pmatrix} I & \\ & -I \end{pmatrix}, \quad \Gamma^\alpha = \begin{pmatrix} \sigma^{\alpha-2} & \\ & -\sigma^{\alpha-2} \end{pmatrix}, \quad (14)$$

with $\alpha=3,4,5$ and σ^μ ($\mu=1,2,3$) are the Pauli matrices. In this new representation, the 2D Luttinger Hamiltonian (10) is also block diagonal:

$$H(\mathbf{k}) = \begin{pmatrix} \epsilon(\mathbf{k}) + Vd_\alpha(\mathbf{k})\sigma^\alpha & \\ & \epsilon(\mathbf{k}) - Vd_\alpha(\mathbf{k})\sigma^\alpha \end{pmatrix}. \quad (15)$$

In other words, the four-component spin-3/2 system is equivalent to a decoupled bilayer QAHE system, each with Hamiltonian (1), but with $d_a(\mathbf{k})$ opposite in the two layers. According to the definition (6), the Hall conductivities of the two layers are opposite to each other. Since Γ^{12} is odd under time-reversal transformation, the two layers are time-reversal partners, and the total Hamiltonian H_{2D} remains time-reversal invariant. The Γ^{12} spin current is given by

$$J_i^\Gamma = J_i^+ - J_i^-, \quad i=x,y, \quad (16)$$

in which $J_i^\pm$ is the current of electrons with $\Gamma^{12}=\pm1$. Thus the Hall conductivity of $J_x^\Gamma=\sigma_{xy}^\Gamma E_y$ is quantized as

$$\sigma_{xy}^\Gamma = \sigma_{xy}^+ - \sigma_{xy}^-$$

$$= -\frac{1}{4\pi^2} \int\int_{\text{FBZ}} dk_x dk_y \hat{\mathbf{d}} \cdot \partial_{\mathbf{x}}\hat{\mathbf{d}} \times \partial_{\mathbf{y}}\hat{\mathbf{d}} \Rightarrow \sigma_{xy}^\Gamma$$

$$= \frac{n}{\pi} \quad (n \in \mathbb{Z}). \quad (17)$$

In general, such a quantized Hall conductivity of the conserved charge Γ^{12} leads to a nonvanishing spin Hall effect in the 2D insulator system (12), which is consistent with the three-dimensional spin Hall insulator model. What is more, the spin Hall transport in the two-dimensional system can be understood better by studying the edge states, as in the QHE and QAHE. To see the picture more clearly, a tight-binding regularization of $d_a(\mathbf{k})$ is specified as

$$d_3(k) = -\sqrt{3}\sin k_x\sin k_y,$$

$$d_4(k) = \sqrt{3}(\cos k_x - \cos k_y),$$

$$d_5(k) = 2 - e_s - \cos k_x - \cos k_y, \quad (18)$$

which reduces to the continuum form in Eqs. (12) when $k_x,k_y\to0$. Direct calculations show that

$$\sigma_{xy}^\Gamma = \begin{cases} 2/\pi, & 0<e_s<4, \\ 0, & e_s>4 \text{ or } e_s<0; \end{cases} \quad (19)$$

thus, the topological charge is 2 when $0<e_s<4$ and t/V is small. The topological charge in this system is larger than the previous QAHE example (7) by one unit, since the d wave functions here "wind around" in the momentum space more than the p-wave functions in the previous QAHE example. In this system there are four edge states on each boundary. For the $\Gamma^{12}=+1(-1)$ states, the $v_y>0$ state is localized on the left (right) edge, while the $v_y<0$ state is localized on the right (left) edge. The energy spectrum and the schematic diagram of the edge states are shown in Fig. 3.

To study the evolution of the edge states in an infinitesimal electric field, we consider the Laughlin-Halperin gauge argument.[13,14] The system with the periodic boundary condition in the y direction and open boundary condition in the x direction can be considered as a cylinder. When the flux $\Phi(t)$ threading the cylinder is adiabatically turned on from $\Phi(0)=0$ to $\Phi(T)=2\pi$, the electric field in the y direction is given by

$$E_y(t) = -\frac{\partial A_y(t)}{\partial t} = \frac{1}{L}\frac{\partial \Phi(t)}{\partial t}. \quad (20)$$

For convenience, the direction of the flux Φ is chosen so that $E_y>0$ when Φ increases. The effect of flux threading can be expressed by replacing $k_y \rightarrow k_y - A_y$ in the Hamiltonian or, equivalently, as a twisted boundary condition $\psi(x,y+L)=e^{i\Phi}\psi(x,y)$. In such a picture, each single-particle eigenstate $\phi_{mk_y}(x,y)=u_{mk_y}(x)e^{ik_y y}$ will be adiabatically transformed into $\phi_{mk_y}(x,y)(t)=u_{m,k_y-A_y}(x)e^{i(k_y-A_y)y}$. In particular, when the flux reaches 2π, the adiabatical evolution will result in

$$|m,k_y\rangle \rightarrow \left|m,k_y+\frac{2\pi}{L}\right\rangle. \quad (21)$$

When the Fermi level lies in the bulk energy gap, the ground state of the system is given by $|G\rangle=\Pi_{E_{mk}\leq\mu}|mk\rangle$. When a 2π flux is threaded through the cylinder, the final state is obtained by a translation of Fermi sea in momentum space: $|G'\rangle=\Pi_{E_{mk}\leq\mu}|m,k+2\pi/L\rangle$. Since the bulk part of $|G\rangle$ is a product of all k's, it does not change under such a translation, which implies that the only difference between $|G\rangle$ and $|G'\rangle$ occurs to the edge states near the Fermi level. As shown in Fig. 3(a) by solid and open circles, near the Fermi level, each edge state on the Fermi surface with velocity $v_y>0$ will move out of the Fermi sea and become a particle excitation since $\delta E \simeq v_y \delta k = 2\pi v_y/L>0$, while each one with $v_y<0$ will move into the Fermi sea and lead to a hole excitation. Consequently, the final state $|G'\rangle$ can be expressed as a particle-hole excitation state as

$$|G'\rangle = \prod_{i=1}^{n} c_{iL+}^{\dagger}c_{iR-}^{\dagger}c_{iL-}c_{iR+}|G\rangle, \quad (22)$$

in which the label $\pm$ stands for the eigenvalue of Γ^{12} carried by the edge state and L and R refer to the edge states on the left and right edges, respectively. n is the bulk topological number. In obtaining Eq. (22), we have used the chirality of the edge states—i.e., $v_{L+}>0, v_{L-}<0, v_{R+}<0, v_{R-}>0$. (A similar analysis of the usual IQHE case can be found in Ref. 25.)

From Eq. (22) it is clear that the net effect of adiabatically turning on a 2π flux is to transfer edge states with $\Gamma^{12}=1$ from the right edge to the left one and to transfer edge states with $\Gamma^{12}=-1$ in the opposite way. This leads to an accumulation of Γ^{12} "spin" on the boundary. Since Γ^{12} is related to S^z by $S^z=-\frac{1}{2}\Gamma^{12}-\Gamma^{34}$ as shown in Ref. 24, such an accumulation of Γ^{12} in general leads to a nonvanishing spin S^z density on the boundary. On the other hand, such an accumulation can also be considered as a consequence of the spin Hall

current j_x induced by the electric field E_y in Eq. (20), which implies that the *physically observed* spin Hall conductivity is proportional to the amplitude of spin accumulation after 2π-flux threading. Since $\langle S^z\rangle=-\frac{1}{2}\langle\Gamma^{12}\rangle-\langle\Gamma^{34}\rangle$, the corresponding spin Hall conductivity also consists of two parts, where the conserved part $\sigma_{xy}^{(c)}=\frac{1}{2}\sigma_{xy}^{\Gamma}$ corresponds to a transport of Γ^{12} spin carried by the motion of edge states, while the nonconserved part $\sigma_{xy}^{(nc)}$ is just a precession effect due to the nonconserved nature of spin as represented by $\langle\Gamma^{34}\rangle$ of each edge state. Consequently, it is only $\sigma_{xy}^{(c)}$ that counts as true transport of quantum states in the system and is protected by the bulk topological structure. These considerations give the physical justification of the conserved spin current operator defined in Ref. 24.

Finally, we consider the effect of breaking the z-axis mirror symmetry, which can be induced by adding an asymmetric potential $U(z)$, such that $U(z) \neq U(-z)$, in the Hamiltonian (10). Consequently, the average $c \equiv \langle k_z\rangle$ in the lowest 2D subband becomes finite. And thus an extra term

$$H_a = V[d_1(\mathbf{k})\Gamma^1 + d_2(\mathbf{k})\Gamma^2] = -\sqrt{3}cV(k_y\Gamma^1+k_x\Gamma^2) \quad (23)$$

should be added to the two-dimensional Hamiltonian (12). Since $\{\Gamma^{12},H_a\}=0$, such a term will lead to a flip between the states with opposite Γ^{12} pseudospin. Especially, a mixing between the left- and right-moving edge states will be induced, and thus a gap $E_{edge}\propto cV$ is open on each edge. Consequently, the system becomes a fully gapped insulator when the chemical potential μ lies within the edge gap; however, the gapless edge excitations still exist if μ is not in the edge gap but remains within the bulk gap. In this case, the spin Hall effect carried by the edge states can still survive, but not as robust as in the fully symmetric case, since it is not completely topology protected.

Spin currents in this spin Hall insulator model has also been discussed in Ref. 26.

IV. CONCLUSIONS AND DISCUSSIONS

In conclusion, we have proposed a topological mechanism for the quantum spin Hall effect, which are realized in a class of two-dimensional spin Hall insulators with mirror symmetry. Mathematically, such a QSHE is the cousin of the quantum Hall effect in band insulators without a magnetic field, the so-called quantum anomalous Hall effect. By carefully studying the Laughlin-Halperin gauge argument, insights are gained into the physical mechanism of the quantum spin Hall transport carried by the edge states. It also provides an understanding of the physical meaning of spin transport in the absence of spin conservation.

The QSHE models discussed in this paper can be experimentally realized in two classes of 2D semiconductors. One class is the (distorted) zero-gap semiconductors such as HgTe, HgSe, β-HgS, and α-Sn. The other class is the narrow-gap semiconductors such as PbTe, PbSe, and PbS.[11] As proposed above, topological quantization of the spin Hall effect shows up in the cases with mirror symmetry with respect to the z axis, realizable when the 2D material is trapped in a symmetric quantum well. Once the quantum spin Hall
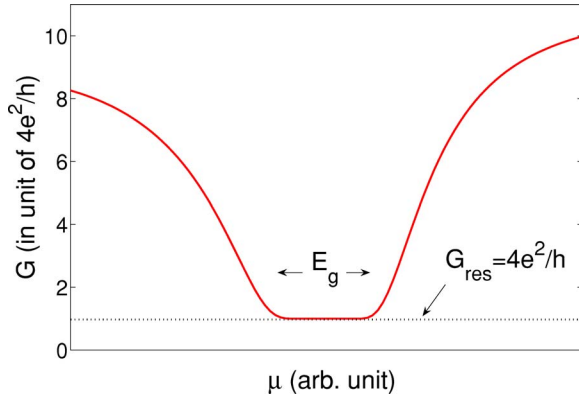
FIG. 4. (Color online) The schematic curve of the conductance G versus Fermi level μ for a ballistic quantum well in the quantum spin Hall regime. The plateau with $G_{res} = \frac{4e^2}{h}$ shows the residual conductance contributed by four edge states on two edges.

effect is realized in the ground state, it is protected against thermal fluctuations by the bulk energy gap E_g. At temperature $T \ll E_g/k_B$, the quantum spin Hall effect is expected to be observable. Take the HgTe/Hg$_{1-x}$Cd$_x$Te (001) quantum well for an example. As calculated in Ref. 27, the gap E_g between LH and HH bands is of the order of 10 meV for $x=0.7$, which means the quantum spin Hall effect can beobserved in a wide temperature range $T \ll 100$ K. Once the spin Hall effect in the pure system is established, it is not significantly dependent on the mobility of the material.

However, the magnitude of edge spin accumulation in a steady state is in general dependent on the spin relaxation mechanism and the disorder in the system. To avoid ambiguity in estimating the edge spin accumulation, here we propose a more definite experimental prediction of the QSHE. As is shown above, there are two pairs of gapless edge states on each boundary, which are chiral in spin transport but *nonchiral* in the charge channel. In other words, each pair of edge states (with opposite Γ^{12} on the same boundary) is equivalent to a *spinless* Luttinger liquid in two-terminal measurements of charge conductance. Consequently, there are in total four pairs of edge states in the system, which will make a quantized contribution,[28]

$$G = \frac{4e^2}{h}, \tag{24}$$

to the longitudinal charge conductance when the system is in a ballistic regime. The schematic curve of longitudinal conductance versus the Fermi level is shown in Fig. 4. Compared to the vanishing conductance in a trivial insulator, such a residual conductance provides a simple probe of the topologically nontrivial edge states in the QSHE.

APPENDIX: KUBO FORMULA CALCULATION OF σ_{xy}

Here we propose a derivation of Eq. (6) from the Kubo formula. The single-particle Green function corresponding to the Hamiltonian (1) can be written as

$$G(\mathbf{k}, i\omega_n) = [i\omega_n - H(\mathbf{k})]^{-1} = \frac{P_+}{i\omega_n - E_+(\mathbf{k})} + \frac{P_-}{i\omega_n - E_-(\mathbf{k})}, \tag{A1}$$

with

$$P_\pm = \frac{1}{2}[1 \pm \hat{d}_\alpha(\mathbf{k})\sigma^\alpha].$$

Then the charge Hall conductivity can be calculated using the Kubo formula (2):

$$
\begin{aligned}
Q_{xy}(i\nu_m) &= \frac{1}{\Omega\beta}\sum_{\mathbf{k},n} \text{tr}[J_x(\mathbf{k})G(\mathbf{k},i(\omega_n+\nu_m))J_y(\mathbf{k})G(\mathbf{k},i\omega_n)] \\
&= \frac{1}{\Omega\beta}\sum_{s,t=\pm}\sum_{\mathbf{k},n} \frac{\text{tr}[J_x(\mathbf{k})P_s(\mathbf{k})J_y(\mathbf{k})P_t(\mathbf{k})]}{[i(\omega_n+\nu_m)-E_s(\mathbf{k})][i\omega_n-E_t(\mathbf{k})]} \\
&= \frac{1}{\Omega}\sum_{s,t=\pm}\sum_{\mathbf{k}} \frac{\text{tr}[J_x(\mathbf{k})P_s(\mathbf{k})J_y(\mathbf{k})P_t(\mathbf{k})]}{i\nu_m-E_s(\mathbf{k})+E_t(\mathbf{k})}[n_t(\mathbf{k})-n_s(\mathbf{k})], \Rightarrow \sigma_{xy} \\
&= \lim_{\omega\to 0}\frac{i}{\omega}Q_{xy}(\omega+i\delta) \\
&= -\frac{i}{\Omega}\sum_{s,t=\pm}\sum_{\mathbf{k}} \frac{\text{tr}[J_x(\mathbf{k})P_s(\mathbf{k})J_y(\mathbf{k})P_t(\mathbf{k})]}{[E_t(\mathbf{k})-E_s(\mathbf{k})]^2}[n_t(\mathbf{k})-n_s(\mathbf{k})] \\
&= -\frac{i}{\Omega}\sum_{\mathbf{k}} \frac{n_-(\mathbf{k})-n_+(\mathbf{k})}{4V^2d(\mathbf{k})^2}\{\text{tr}[J_x(\mathbf{k})P_+(\mathbf{k})J_y(\mathbf{k})P_-(\mathbf{k})]-\text{H.c.}\}. \tag{A2}
\end{aligned}
$$

Here $E_{\pm}(\mathbf{k}) = \epsilon(\mathbf{k}) \pm V d(\mathbf{k})$ is introduced in the last line. The trace in Eq. (A2) can be worked out by substituting $J_{x,y}(\mathbf{k})$ and $P_{\pm}(\mathbf{k})$ by their definition (3) and (A1), respectively:

$$\sigma_{xy} = \frac{i}{4\Omega} \sum_k \text{Tr} \left\{ \left(\frac{\partial \epsilon(k)}{\partial k_x} + V \frac{\partial d_\alpha(k)}{\partial k_x} \sigma^\alpha \right) (1 - \hat{d}_\alpha \sigma^\alpha) \left(\frac{\partial \epsilon(k)}{\partial k_y} + V \frac{\partial d_\alpha(k)}{\partial k_y} \sigma^\alpha \right) (1 + \hat{d}_\alpha \sigma^\alpha) - \text{H.c.} \right\} \frac{n_-(\mathbf{k}) - n_+(\mathbf{k})}{4 V^2 d^2}$$

$$= -\frac{1}{2\Omega} \sum_k \left\{ \frac{\partial \hat{d}_\alpha(k)}{\partial k_x} \frac{\partial \hat{d}_\beta(k)}{\partial k_y} \hat{d}_\gamma \epsilon^{\alpha\beta\gamma} \right\} [n_-(\mathbf{k}) - n_+(\mathbf{k})]. \tag{A3}$$

For the last step, it should be noticed that only the 3-σ^α terms in the expansion make a nonvanishing contribution to the trace. Thus the final result is independent of coupling V, as expected from topological considerations. This finishes our derivation of formula (4) for the spin Hall conductance.

---

[1] S. Murakami, N. Nagaosa, and S. C. Zhang, Science **301**, 1348 (2003).

[2] J. Sinova, D. Culcer, Q. Niu, N. A. Sinitsyn, T. Jungwirth, and A. H. MacDonald, Phys. Rev. Lett. **92**, 126603 (2004).

[3] J. I. Inoue, G. E. W. Bauer, and L. W. Molenkamp, Phys. Rev. B **70**, 041303 (2004).

[4] R. Raimondi and P. Schwab, Phys. Rev. B **71**, 033311 (2005).

[5] E. G. Mishchenko, A. V. Shytov, and B. I. Halperin, Phys. Rev. Lett. **93**, 226602 (2004).

[6] S. Murakami, Phys. Rev. B **69**, 241202(R) (2004).

[7] B. A. Bernevig and S.-C. Zhang, Phys. Rev. Lett. **95**, 016801 (2005).

[8] W. Q. Chen, Z. Y. Weng, and D. N. Sheng, Phys. Rev. Lett. **95**, 086605 (2005).

[9] Y. K. Kato, R. C. Myers, A. C. Gossard, and D. D. Awschalom, Science **306**, 1910 (2004).

[10] J. Wunderlich, B. Kaestner, J. Sinova, and T. Jungwirth, Phys. Rev. Lett. **94**, 047204 (2005).

[11] S. Murakami, N. Nagaosa, and S.-C. Zhang, Phys. Rev. Lett. **93**, 156804 (2004).

[12] B. A. Bernevig and S.-C. Zhang, Phys. Rev. Lett. **96**, 106802 (2005).

[13] R. B. Laughlin, Phys. Rev. B **23**, 5632 (1981).

[14] B. I. Halperin, Phys. Rev. B **25**, 2185 (1982).

[15] D. N. Sheng, L. Sheng, Z. Y. Weng, and F. D. M. Haldane, Phys. Rev. B **72**, 153307 (2005).

[16] F. D. M. Haldane, Phys. Rev. Lett. **61**, 2015 (1988).

[17] C. L. Kane and E. J. Mele, Phys. Rev. Lett. **95**, 226801 (2005).

[18] D. J. Thouless, M. Kohmoto, M. P. Nightingale, and M. den Nijs, Phys. Rev. Lett. **49**, 405 (1982).

[19] V. M. Yakovenko, Phys. Rev. Lett. **65**, 251 (1990).

[20] M. Kohmoto, Ann. Phys. (N.Y.) **160**, 355 (1985).

[21] Q. Niu, D. J. Thouless, and Y.-S. Wu, Phys. Rev. B **31**, 3372 (1985).

[22] G. Volovik, *The Universe in a Helium Droplet* (Oxford University Press, Oxford, 2003).

[23] J. M. Luttinger, Phys. Rev. **102**, 1030 (1956).

[24] S. Murakami, N. Nagaosa, and S.-C. Zhang, Phys. Rev. B **69**, 235206 (2004).

[25] Y. Hatsugai, Phys. Rev. B **48**, 11851 (1993).

[26] M. Onoda and N. Nagaosa, Phys. Rev. Lett. **95**, 106601 (2005).

[27] E. G. Novik, A. Pfeuffer-Jeschke, T. Jungwirth, V. Latussek, C. R. Becker, G. Landwehr, H. Buhmann, and L. W. Molenkamp, Phys. Rev. B **72**, 035321 (2005).

[28] D. L. Maslov and M. Stone, Phys. Rev. B **52**, R5539 (1995).